UNSTEADY MHD BIO-NANOCONVECTIVE ANISTROPIC SLIP FLOW PAST A VERTICAL ROTATING CONE

by

Nur Amalina ABDUL LATIFF [a], Mohammed Jashim UDDIN [b*], and Ahmad Izani MD. ISMAIL [c]

[a] School of Mathematical Sciences, Universiti Sains Malaysia, 11800, Penang, Malaysia.
[b] Professor and Head of Mathematics Department, American International University-Bangladesh, Banani, Dhaka, Bangladesh.
*Corresponding Author Email: jashim_74@yahoo.com

MHD bioconvective of nanofluid flow past a rotating cone with anistropic velocity slips, thermal slip, mass slip and microorganism slips is studied theoretically and numerically. Suitable similarity transformations are used to transform the governing boundary layer equations into non-linear ordinary differential equations which were then solved numerically. The effect of the governing parameters on the dimensionless velocities, temperature, nanoparticle volume fraction (concentration), density of motile microorganisms as well as on the local skin friction, local Nusselt, Sherwood number and the local motile microorganism numbers are examined. Results from this investigation were compared with previous related investigations and good agreement was found. It is found that for both in the presence and absence of magnetic field, increasing velocity slips reduce the friction factor. It is also found that increasing thermal slip, mass slip and microorganism slips strongly reduce heat, mass and microorganism transfer respectively. This study is relevant in bio-chemical industries in which microfluidic devices involved.

Keywords: *Rotating cone; anistropic slip; MHD; microorganisms*

Introduction

The study of boundary layer flow, heat and mass transfer involving rotating cones has attracted many researchers due to wide applications in the automobile and chemical industries. These industries extensively use rotating heat exchangers [1]. Spin stabilized missiles, containers of nuclear waste disposal and geothermal reservoirs are also some of the applications of rotating cones [1,3]. The heat and mass transfer characteristics of cone bodies can be described by obtaining a self-similar solution of boundary layer flows. Similar solutions for cone geometries exist when temperature is considered to vary as a power function of distance along a cone ray [4]. Many studies have been communicated deploying numerical and analytical methods to study various aspects of rotating cone problem [2], [4], [5] and [6]. Raju [7] has considered the influences of the thermophoresis and thermal radiation on mixed convection heat and mass transfer phenomena past a vertical rotating cone in a fluid saturated porous medium. Nadeem and Saleem [8] have investigated the effects of thermophoresis and Brownian motion on the heat and mass transfer of third grade nanofluid flow over a rotating vertical cone. Hashmi et al. [9] stated that fluid flow incorporating a magnetic field avoids the adverse impact of temperature on lubrication viscosity under extreme operating conditions. Nadeem and Saleem [10] applied the homotopy analysis method to examine the combined effects of buoyancy force and the magnetic field on a rotating cone body in a rotating frame. Nadeem and Saleem [3] analyzed the heat and mass transfer effects of MHD mixed convection flow of rotating nanofluids over a rotating cone. Recent relevant study can be found in references [11–18].

Slip conditions exist on hydrophobic surfaces such as in microfluidics and nanofluidics devices used in microelectromechanical systems and nanoelectromechanical systems [19]. Thus, many researchers are interested to investigate the various aspects of fluid flow, heat and mass transfer with velocity slip boundary conditions under various geometries and using various solution methods ([20],

[21], [22], [23], [24], [25], [26], [27], [28] and [29]). In the case of multiple slips boundary conditions under various geometries, Uddin et al. [30] analyzed the influence of variable transport properties, momentum, thermal, and mass slip on MHD momentum, heat, and mass transfer in a Darcian porous medium. Uddin et al. [31] studied the effects of temperature dependent viscosity and thermal conductivity and concentration dependent mass diffusivity on the electrically conducting Newtonian fluid flow along a moving stretching sheet embedded in a porous medium. Also, studies have been conducted on micro-scale devices focusing on slip flow over a rotating cone ([32], [15] and [14]). Most of the previous researchers used isotropic slip boundary conditions. In this paper we use anisotropic slip boundary conditions to get realistic results [23].

An innovation can be made to microfluidic devices by taking into account nanofluids and bioconvection. Bioconvection occurs due to the collective swimming of motile microorganisms in a particular direction and hence increasing the density of the base fluid [33]. Nield and Kuznetsov [34] stated that microorganisms can contribute toward the improvement in biomicrosystems since they play an important role in mass transport enhancement and mixing because traditional active mixers used are expensive and energy-intensive for fabrication. Some recent studies dealt with bioconvection phenomena under various geometries effect include Shen et al. [35] and Sameh et al. [36]. A recent study of bioconvection phenomena in rotating cone was conducted by Raju [37] who analyzed the heat and mass transfer of bioconvection non-Newtonian fluid flow over a rotating cone/plate taking into account nonlinear thermal radiation and chemical reaction.

Therefore, the aim of this study is to extend the work of Saleem and Nadeem [14] by combining the effects of multiple slips, magnetic field, nanofluids, bioconvection and rotating cone geometry. We apply the similarity variables to get the similarity equations and then solve them using the shooting method in Maple. The influences of various physical parameters on the velocity, temperature, concentration and microorganism fields are explored in detail. In addition, the effects of the emerging parameters on surface shear stress, wall heat, mass and microorganism transfer rate are also studied in detail. We believe that it can contribute a significant role to enhance heat, mass and microorganism transfer rate in micro-fluidic bio-devices application.

Mathematical formulations of the problem

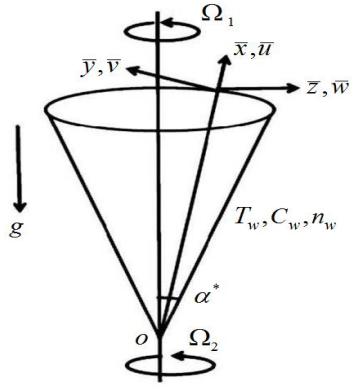

Figure 1. Schematic diagram of vertical rotating cone

Consider the unsteady, axi-symmetric, rotating cone of nanofluids flow with microorganisms. It is assumed that rotating cone with velocity as a function of time develops unsteadiness in the flow field. Also, it is assumed that the rectangular curvilinear coordinate system is fixed. The temperature, mass and microorganisms difference in the flow field induce the existence of the buoyancy forces. The velocity components along the $\bar{x}$, $\bar{y}$ and $\bar{z}$ directions are represent by $\bar{u}$, $\bar{v}$ and $\bar{w}$ respectively. A magnetic field normal to the rotating cone is applied. A schematic of the physical configuration is shown in Fig. 1 which follows the work of Saleem and Nadeem [14]. Inside the boundary layer, the fluid temperature, the nanoparticle volume friction and the density of motile microorganisms represent by T, C and n respectively. At the wall, the temperature, nanoparticle volume friction and density of motile microorganisms represent by T_w, C_w and n_w respectively and far away from the wall they are

represent using T_∞ , C_∞ and n_∞ respectively. By using these assumptions, the time-dependent governing equations for mass, momentum in the $\bar{x}$ - and $\bar{z}$ -directions, energy, concentration and microorganism conservation are given by:

$$\frac{\partial \bar{u}}{\partial \bar{x}} + \frac{\bar{u}}{\bar{x}} + \frac{\partial \bar{w}}{\partial \bar{z}} = 0, \tag{1}$$

$$\frac{\partial \bar{u}}{\partial \bar{t}} + \bar{u}\frac{\partial \bar{u}}{\partial \bar{x}} + \bar{w}\frac{\partial \bar{u}}{\partial \bar{z}} - \frac{\bar{v}^2}{\bar{x}} = \frac{\mu}{\rho_f}\left(\frac{\partial^2 \bar{u}}{\partial \bar{z}^2}\right) + \frac{1}{\rho_f}\begin{bmatrix}(1-C_\infty)\rho_{f\infty}\beta g(T-T_\infty)\\ -(\rho_p-\rho_{f\infty})g(C-C_\infty)\\ -(n-n_\infty)g\gamma(\rho_m-\rho_{f\infty})\end{bmatrix} - \frac{\sigma B^2}{\rho_f}\bar{u}, \tag{2}$$

$$\frac{\partial \bar{v}}{\partial \bar{t}} + \bar{u}\frac{\partial \bar{v}}{\partial \bar{x}} + \bar{w}\frac{\partial \bar{v}}{\partial \bar{z}} - \frac{\bar{u}\,\bar{v}}{\bar{x}} = \frac{\mu}{\rho}\left(\frac{\partial^2 \bar{u}}{\partial \bar{z}^2}\right) - \frac{\sigma B^2}{\rho_f}\bar{v}, \tag{3}$$

$$\frac{\partial T}{\partial \bar{t}} + \bar{u}\frac{\partial T}{\partial \bar{x}} + \bar{w}\frac{\partial T}{\partial \bar{z}} = \alpha\frac{\partial^2 T}{\partial \bar{z}^2} + \tau D_B\frac{\partial T}{\partial \bar{z}}\frac{\partial C}{\partial \bar{z}} + \tau\frac{D_T}{T_\infty}\left(\frac{\partial T}{\partial \bar{z}}\right)^2, \tag{4}$$

$$\frac{\partial C}{\partial \bar{t}} + \bar{u}\frac{\partial C}{\partial \bar{x}} + \bar{w}\frac{\partial C}{\partial \bar{z}} = D_B\frac{\partial^2 C}{\partial \bar{z}^2} + \frac{D_T}{T_\infty}\frac{\partial^2 T}{\partial \bar{z}^2}, \tag{5}$$

$$\frac{\partial n}{\partial \bar{t}} + \bar{u}\frac{\partial n}{\partial \bar{x}} + \bar{w}\frac{\partial n}{\partial \bar{z}} + \frac{b^{*}W_c}{C_w - C_\infty}\left[\frac{\partial}{\partial \bar{z}}\left(n\frac{\partial C}{\partial \bar{z}}\right)\right] = D_n\left(\frac{\partial^2 n}{\partial \bar{z}^2}\right). \tag{6}$$

where $\bar{t}$ is the time, μ is the fluid viscosity, g is the acceleration due to gravity, ρ is the fluid density, β is the volumetric thermal expansion coefficient of the base fluid, α is the fluid thermal diffusivity, γ is the average volume of a microorganism, ρ_m is the microorganisms density, τ is the ratio of heat capacity of nanoparticle and heat capacity of fluid, D_B is the Brownian diffusion coefficient, D_T is the thermophoretic diffusion coefficient, b^{*} is the chemotaxis constant, W_C is the maximum cell swimming speed and D_n is the microorganism diffusivity coefficient. We assumed that the cone is subjected to $\bar{u}-$ and $\bar{v}-$velocity, thermal, mass and microorganism slip, the boundary conditions become [26][14]:

$$\begin{aligned}
&\bar{w} = 0,\ \bar{u} = N_1(\bar{x},\bar{t})\nu\left(\frac{\partial \bar{u}}{\partial \bar{z}}\right),\ \bar{v} = N_2(\bar{x},\bar{t})\nu\left(\frac{\partial \bar{v}}{\partial \bar{z}}\right) + \bar{x}\left(\Omega\sin\alpha\right)\left(1 - s\left(\Omega\ \sin\alpha\right)\bar{t}\right)^{-1},\\
&T = T_w(\bar{x},\bar{t}) + D(\bar{x},\bar{t})\left(\frac{\partial T}{\partial \bar{z}}\right),\ C = C_w(\bar{x},\bar{t}) + E(\bar{x},\bar{t})\left(\frac{\partial C}{\partial \bar{z}}\right),\\
&n = n_w(\bar{x},\bar{t}) + F(\bar{x},\bar{t})\left(\frac{\partial n}{\partial \bar{z}}\right) \text{ at } \bar{y} = 0,\\
&\bar{u} = 0,\ \bar{v} = 0,\ \bar{T} \to \bar{T}_\infty,\ \bar{C} \to \bar{C}_\infty,\ \bar{n} \to 0 \text{ as } \bar{y} \to \infty.
\end{aligned} \tag{7}$$

Similarity Transformations

To proceed, we introduce the following transformations [14]:

$$\eta=\left(\frac{\Omega\sin\alpha^*}{\nu}\right)^{\frac{1}{2}}(1-st)^{-\frac{1}{2}}\,\bar{z},\ \ \bar{u}=-\frac{1}{2}\Omega\,\bar{x}\sin\alpha^*(1-st)^{-1}\,f'(\eta),$$

$$\bar{v}=\Omega\,\bar{x}\sin\alpha^*(1-st)^{-1}\,g(\eta),\ \ \bar{w}=\left(\nu\,\Omega\sin\alpha^*\right)^{\frac{1}{2}}(1-st)^{-\frac{1}{2}}\,f(\eta),$$

$$T=T_\infty+(T_w-T_\infty)\theta(\eta),\ T_w-T_\infty=\left((T_w)_0-T_\infty\right)\left(\frac{\bar{x}}{L}\right)(1-st)^{-2},\tag{8}$$

$$C=C_\infty+(C_w-C_\infty)\phi(\eta),\ C_w-C_\infty=\left((C_w)_0-C_\infty\right)\left(\frac{\bar{x}}{L}\right)(1-st)^{-2},$$

$$n=n_w\,\chi(\eta),\ n_w=(n_w)_0\left(\frac{\bar{x}}{L}\right)(1-st)^{-2},\ B(\bar{x},\bar{t})=B_0\sin\alpha^*(1-st)^{-1},$$

$$t=\left(\Omega\sin\alpha^*\right)\bar{t}.$$

Using (8), we have transformed Eqns. (1)-(7) into a system of ordinary differential equations:

$$f'''-f\,f''+\frac{1}{2}f'^2-2g^2-s\left[f'+\frac{1}{2}\eta f''\right]-2\lambda\left[\theta-Nr\,\phi-Rb\,\chi\right]-M\,f'=0\tag{9}$$

$$g''-f\,g'+f'g-s\left(g+\frac{1}{2}\eta g'\right)-M\,g=0\tag{10}$$

$$\theta''-\Pr\left[s\left(\frac{1}{2}\eta\theta'+2\theta\right)-\frac{1}{2}f'\theta+f\,\theta'\right]+Nb\,\theta'\phi'+Nt\,\theta'^2=0,\tag{11}$$

$$\phi''-Sc\left[s\left(\frac{1}{2}\eta\phi'+2\phi\right)-\frac{1}{2}f'\phi+f\,\phi'\right]+\frac{Nb}{Nt}\theta''=0,\tag{12}$$

$$\chi''-Sb\left[s\left(\frac{1}{2}\eta\,\chi'+2\chi\right)-\frac{1}{2}f'\chi+f\,\chi'\right]-Pe\left(\phi''+\phi'\chi'\right)=0,\tag{13}$$

subjected to the boundary conditions:

$$\begin{aligned}&f(0)=0,\ \ f'(0)=\delta_u\,f''(0),\ \ g(0)=1+\delta_v\,g'(0),\\&\theta(0)=1+\delta_T\,\theta'(0),\ \ \phi(0)=1+\delta_C\,\phi'(0),\ \ \chi(0)=1+\delta_n\,\chi'(0),\\&f'(+\infty)=g(+\infty)=\theta(+\infty)=\phi(+\infty)=\chi(+\infty)=0,\end{aligned}\tag{14}$$

Here parameters are defined as $Nr=\dfrac{(C_0-C_\infty)(\rho_o-\rho_f)}{\beta(T_0-T_\infty)(1-C_\infty)\rho_f}$ (buoyancy ratio), $Rb=\dfrac{\gamma\,n_0(\rho_m-\rho_f)}{\beta(T_0-T_\infty)(1-C_\infty)\rho_f}$ (bioconvection Rayleigh number), $\Pr=\dfrac{\nu}{\alpha}$ (Prandtl number), $Sc=\dfrac{\nu}{D_B}$ (Schmidt number), $Sb=\dfrac{\nu}{D_m}$ (bioconvection Schmidt number), $Pe=\dfrac{\beta W_c}{D_m}$ (bioconvection Péclet number), $\lambda=\dfrac{Gr}{\mathrm{Re}_L^2}$ (mixed

convection) where $Gr = g\beta\cos\alpha^*\left(T_0 - T_\infty\right)\left(1-C_\infty\right)\frac{L^3}{\nu^2}$ (Grashoff number) and $\mathrm{Re}_L^2 = \Omega\sin\alpha^*\frac{L^2}{\nu}$ (Rayleigh number), $M^2 = \frac{\sigma B_0^2}{\rho_f}\frac{1}{\Omega}$ (magnetic field), $Nb = \frac{\tau D_B \Delta C}{\alpha}$ (Brownian motion), $Nt = \frac{\tau D_T \Delta T}{\alpha T_\infty}$ (thermophoresis), $\delta_u = \left(N_1\right)_0 \nu^{\frac{1}{2}}\left(\Omega\sin\alpha^*\right)^{\frac{1}{2}}\left(1-st\right)^{-\frac{1}{2}}$ (*u*-velocity slip), $\delta_v = \left(N_2\right)_0 \nu^{-\frac{1}{2}}\left(\Omega\sin\alpha^*\right)^{\frac{1}{2}}\left(1-st\right)^{-\frac{1}{2}}$ (*v*-velocity slip), $\delta_T = D_0 \nu^{-\frac{1}{2}}\left(\Omega\sin\alpha^*\right)^{\frac{1}{2}}\left(1-st\right)^{-\frac{1}{2}}$ (thermal slip), $\delta_C = E_0 \nu^{-\frac{1}{2}}\left(\Omega\sin\alpha^*\right)^{\frac{1}{2}}\left(1-st\right)^{-\frac{1}{2}}$ (mass slip) and $\delta_n = F_0 \nu^{-\frac{1}{2}}\left(\Omega\sin\alpha^*\right)^{\frac{1}{2}}\left(1-st\right)^{-\frac{1}{2}}$ (microorganisms slip).

Physical quantities

The quantities of practical interest are the local skin friction in primary and secondary directions, the local Nusselt number, local Sherwood number and the local wall motile microorganism number. These are respectively, defined by:

$$
\begin{aligned}
&C_{f\bar{x}} = \frac{\tau_{\bar{x}\bar{z}}\big|_{\bar{z}=0}}{\rho_f\left(\Omega\bar{x}\sin\alpha^*\left(1-s\bar{t}\right)^{-1}\right)^2},\ C_{f\bar{y}} = \frac{\tau_{\bar{y}\bar{z}}\big|_{\bar{z}=0}}{\rho_f\left(\Omega\bar{x}\sin\alpha^*\left(1-s\bar{t}\right)^{-1}\right)^2},\\
&Nu_{\bar{x}} = \frac{\bar{x}\,q_w}{k(\bar{T}_w-\bar{T}_\infty)},\ Sh_{\bar{x}} = \frac{\bar{x}\,m_w}{D_B(\bar{C}_w-\bar{C}_\infty)},\ Q_{n\bar{x}} = \frac{\bar{x}\,q_n}{D_n\bar{n}_w},
\end{aligned}
\tag{15}
$$

where $\tau_{\bar{x}\bar{z}}$, q_w, m_w and q_n represent the shear stress in primary and secondary directions, surface heat flux, surface mass flux and the surface motile microorganism flux respectively. These quantities are defined as follows:

$$
\begin{aligned}
&\tau_{\bar{x}\bar{z}} = \mu\left[\frac{\partial\bar{u}}{\partial\bar{z}}\right]_{\bar{z}=0},\ \tau_{\bar{y}\bar{z}} = \mu\left[\frac{\partial\bar{v}}{\partial\bar{z}}\right]_{\bar{z}=0},\ q_w = -k\left[\frac{\partial\bar{T}}{\partial\bar{z}}\right]_{\bar{z}=0},\ m_w = -D_B\left[\frac{\partial\bar{C}}{\partial\bar{z}}\right]_{\bar{z}=0},\\
&q_n = -D_n\left[\frac{\partial\bar{n}}{\partial\bar{z}}\right]_{\bar{z}=0}.
\end{aligned}
\tag{16}
$$

The local skin friction in primary and secondary directions, the local Nusselt number, local Sherwood number and the local wall motile microorganism number in dimensionless form are:

$$
\begin{aligned}
&0.5C_{f\bar{x}}\,\mathrm{Re}_{\bar{x}}^{1/2} = -f''(0),\ \ 0.5C_{f\bar{y}}\,\mathrm{Re}_{\bar{x}}^{1/2} = -g'(0),\ \ Nu_{\bar{x}}\,\mathrm{Re}_{\bar{x}}^{-1/2} = -\theta'(0),\\
&Sh_{\bar{x}}\,\mathrm{Re}_{\bar{x}}^{-1/2} = -\phi'(0),\ \ Q_{n\bar{x}}\,\mathrm{Re}_{\bar{x}}^{-1/2} = -\chi'(0).
\end{aligned}
\tag{17}
$$

Here, $\mathrm{Re}_{\bar{x}} = \Omega\bar{x}^2\sin\alpha^*\left(1-s\bar{t}\right)^{-1}/\nu$ is the local Reynolds number.

Numerical solutions and validation

It is important to note that in the absence of microorganism equation (Eq. 13), without magnetic field and slips, our problem reduces to the problem investigated by Saleem and Nadeem [14]. It is also noticed that in the absence of microorganism equation, without magnetic field and slips and also considering cone is rotating either in an ambient fluid or rotating with equal angular velocity

in the same direction, this paper reduces to problem investigated by Anilkumar and Roy [1]. We used the shooting procedure in Maple to solve the transformed equations. In order to validate our results, we compare our numerical results with Anilkumar and Roy [1]. The comparison in listed in Table 1 and shows a good agreement between these two results.

Table 1: Comparison of the skin friction in the *x*-, *y*-direction and heat transfer in the absence of concentration, microorganism equations and for values for $\delta_u = \delta_v = \delta_T = \delta_C = \delta_n = s = 0$.

Pr	λ	Present			Anilkumar and Roy [1]		
		$-f''(0)$	$-g'(0)$	$-\theta'(0)$	$-f''(0)$	$-g'(0)$	$-\theta'(0)$
0.7	0.0	1.0205	0.6159	0.4287	1.0199	0.6160	0.4305
	1.0	2.0789	0.8508	0.6120	2.1757	0.8499	0.6127
1.0	0.0	1.0204	0.6159	0.5180	1.0199	0.6160	0.5181
	1.0	2.0039	0.8249	0.7005	2.0627	0.8250	0.7005

Results and discussions

For the simulations, we consider water based nanofluid Pr=6.8 (water), Nb=Nt=Nr= $1e^{-5}$, λ =1 (mixed convection) and *s*=0.5. The numerical results of various parameters such as *Sc*, *Sb*, *Pe*, δ_u, δ_v, δ_T, δ_C and δ_n on the dimensionless velocity in the *x*- and *y*-directions, temperature, nanoparticle volume fraction, microorganism are plotted over η which are plotted in Figs. 2-8. Figs. 2(a) to 2(e) show the effects of δ_u on the dimensionless velocity in the *x*- and *y*-directions, temperature, nanoparticle volume fraction and microorganism profiles for different cases of magnetic field parameter (with magnetic or without magnetic). Increasing velocity slip is due to high acceleration of nanofluid and hence it tends to effect nanofluid to slip near the wall. This phenomenon can be observed in Fig. 2(a) where δ_u with higher magnitude gives overshoot value on velocity along *x*-axis $(-f(\eta))$. However, it is observed in Fig. 2(b) that increasing of δ_u reduces the velocity along the *y*-axis $(g(\eta))$. The influence of the magnetic field, M and slip parameter, δ_u is to reduce the velocity in the *y*-axis. Fig. 2(c) reveals that increasing δ_u, the temperature is decreased without magnetic field effect. The high acceleration of nanofluids occurs due to enhance of δ_u. Therefore, it simultaneously cools the boundary layer and hence decreases thermal boundary layer thickness. Figs. 2(d) and 2(e) show the effects of δ_u and M on the nanoparticle volume fraction and microorganism respectively. Both functions follow the same trends as temperature distributions. With greater magnitude of δ_u, both the nanoparticle volume fraction and microorganism concentration profiles are

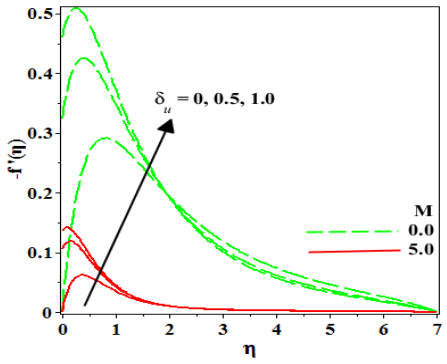

2(a)

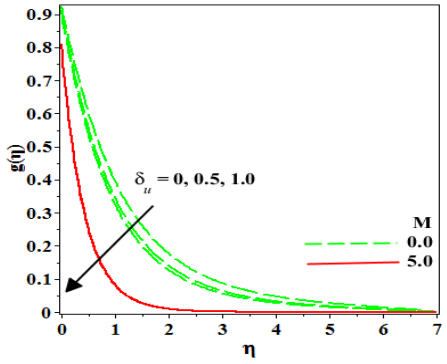

2(b)

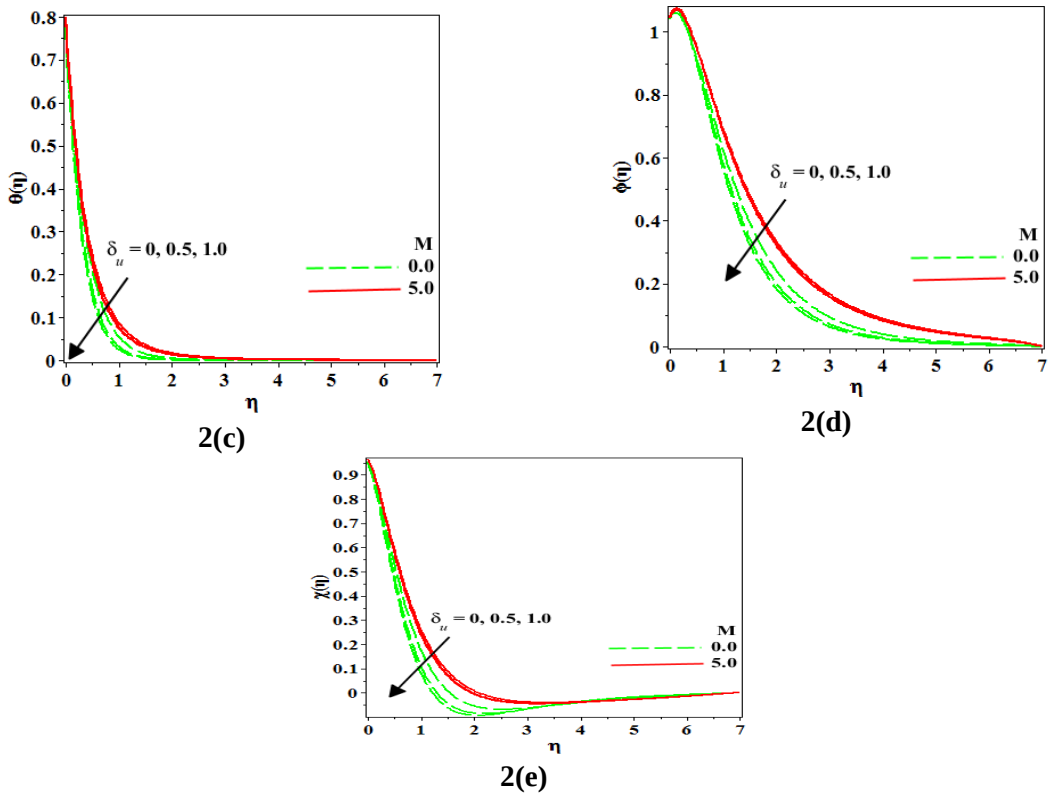

Figures 2. The effects of δ_u and M on the dimensionless (a) velocity in the *x*-direction, (b) velocity in the y-direction, (c) temperature, (d) nanoparticle volume fractions and (e) microorganism profiles when $Sb = Sc = 0.1,\ Pe = \lambda = Rb = 0.1,$ and $\delta_v = \delta_T = \delta_C = \delta_n = 0.1.$

decreased. It is should be mentioned that the motion of motile microorganisms is considered as being independent from the motion of nanoparticles. The motion of nanoparticle volume fraction is due to the Brownian motion in the nanofluids.

Figs. 3(a) to 3(e) represent the effects of δ_v and magnetic field on the dimensionless velocity in the *x*- and *y*-directions, temperature, nanoparticle volume fraction, microorganism respectively. It can be found in Figs. 3(a) and 3(b) that greater δ_v induces flow to decelerate in *x*- and *y*- directions. Therefore, the combined effect of increasing δ_v and the magnetic field causes the temperature to be increased (Fig. 3(c)). Figs. 3(d) and 3(e) show the effects of δ_v and M on the nanoparticle volume fraction and microorganism respectively. Both functions follow the same trend as the temperature distribution. With greater magnitude of δ_v, both the nanoparticle volume fraction and microorganism concentration profiles are increased. As earlier, increasing δ_u is found to suppress both nanoparticle volume fraction and microorganism whereas increasing δ_v generally increases them.

Figs. 4(a) to 4(e) illustrate the effects of thermal slip, δ_T on the velocities, temperature, nanoparticle volume fraction and microorganism with magnetic field. Greater thermal slip is found to decelerate flow in *x*-direction and accelerate flow in *y*-direction. From Fig. 4(a) it can be seen that greater thermal slip with no magnetic field effect significantly suppress the *x*-direction velocity and overshoot near the wall. When the flow passes the nearest surface, the temperature profile significantly reduces toward the free stream. However, velocity of fluid in *y*-direction with no magnetic field effect increases as the δ_T increases. Figs.4(c) to 4(e) presents the reduced values of temperature, nanoparticle volume fraction and microorganism profiles as thermal slip increases.

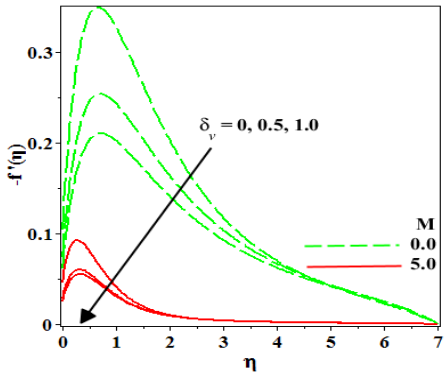

3(a)

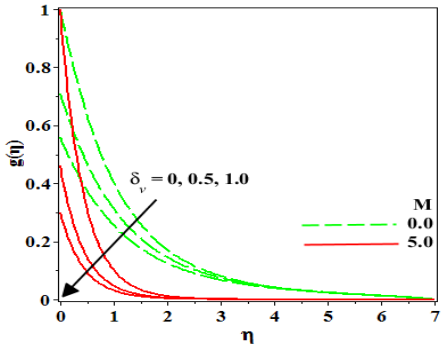

3(b)

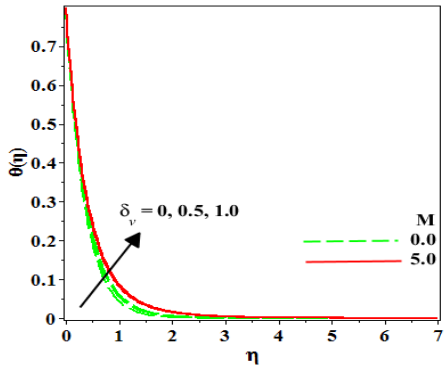

3(c)

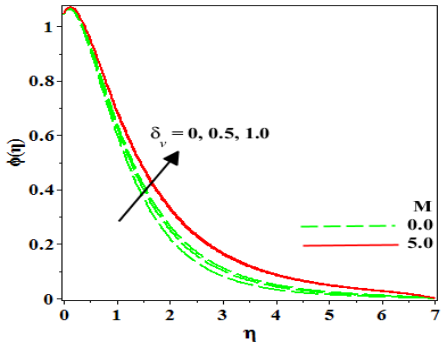

3(d)

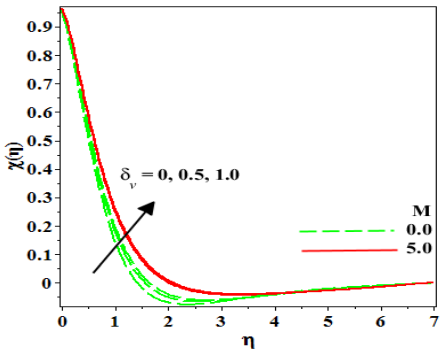

3(e)

Figures 3. The effects δ_v and *M* on the dimensionless (a) velocity in the *x*-direction, (b) velocity in the *y*-direction, (c) temperature, (d) nanoparticle volume fraction and (e) microorganism profiles when $Sb = Sc = 0.1,\ Pe = \lambda = Rb = 0.1,$ and $\delta_u = \delta_T = \delta_C = \delta_n = 0.1.$

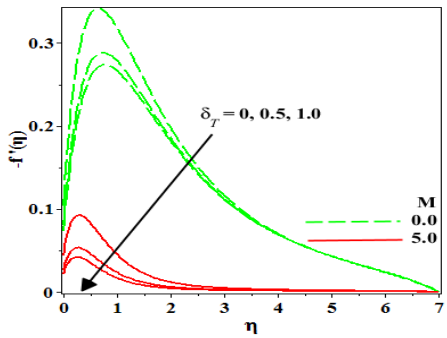

4(a)

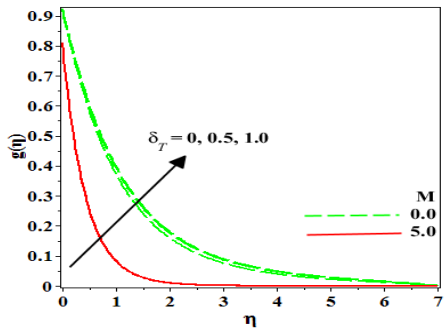

4(b)

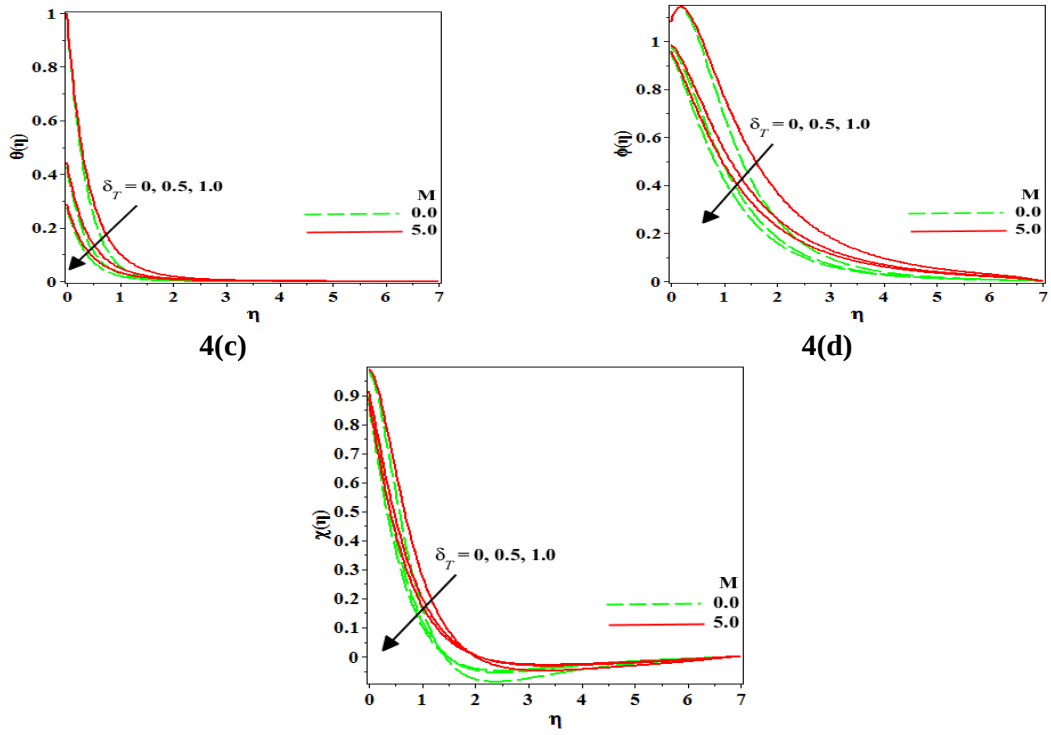

Figures 4. The effects of δ_T and M on the dimensionless (a) velocity in the x-direction, (b) velocity in the y-direction, (c) temperature, (d) nanoparticle volume fraction and (e) microorganism profiles when $Sb = Sc = Pe = \lambda = 0.1,\ Rb = 0.1,$ and $\delta_u = \delta_v = \delta_C = \delta_n = 0.1.$

Based on Fig. 5(a), nanoparticle volume fraction concentrations are maximum at the wall as greater mass slip present. However, there is no significant different on nanoparticle volume fraction values near the wall as M is induced. In Fig. 5(b), microorganism concentrations are conversely reducing its value as mass slip increases. Overall, both nanoparticles volume fraction and microorganisms function show no significant different near the wall as magnetic field increases. It is important to mention that the effect of mass slip on dimensionless velocities and temperature are not significant. Fig. 6 illustrated the combined effect of microorganism slip and magnetic field on the dimensionless microorganism concentration. It can be found that with increasing microorganism slip, the dimensionless microorganism concentration profile decreases. Overall, magnetic field effect with no microorganism slip contributes a factor for dimensionless microorganism concentration to enhance. Also, there is no significant effect occurred on velocities, temperature and nanoparticle volume fraction as microorganism slip increases.

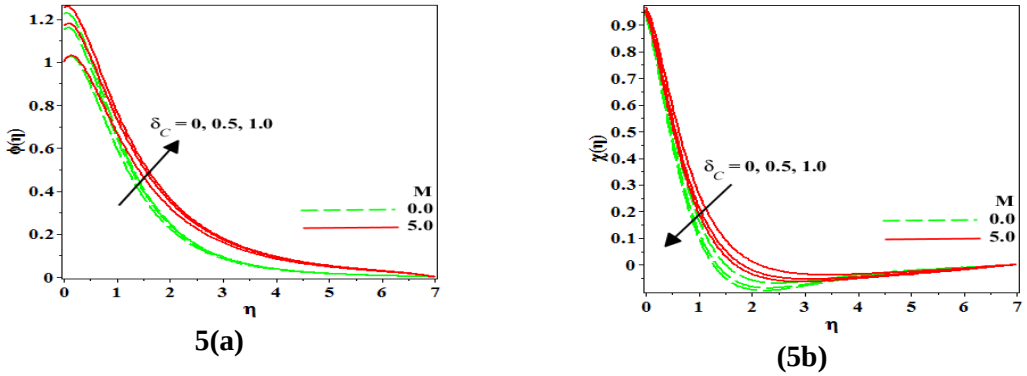

Figures 5. The effects of δ_C and M on the dimensionless (a) nanoparticle volume fraction and (b) microorganism profiles when $Sb = Sc = Rb = Pe = \lambda = 0.1,$ and $\delta_u = \delta_v = \delta_T = \delta_n = 0.1.$

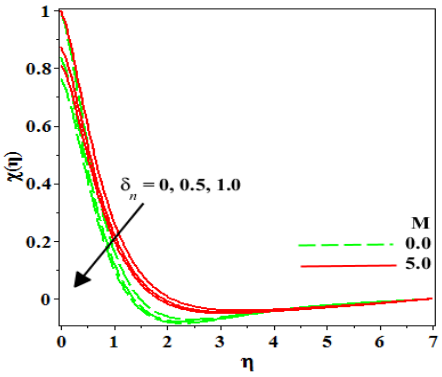

Figure 6. The effects of δ_n and M on the dimensionless microorganism profile when $Sb = Sc = Rb = Pe = \lambda = 0.1,$ and $\delta_u = \delta_v = \delta_T = \delta_C = 0.1.$

Figs. 7(a) and (b) depict the effects of Schmidt number and magnetic field on the dimensionless nanoparticle volume fraction and microorganism profiles. Physically, there are two situations which occur as Schmidt (*Sc*) number increases. There is either lower solutal diffusivity for a uniform fluid dynamic viscosity or higher dynamic viscosity for uniform solutal diffusivity. Fig. 7(a) shows that as the Schmidt number increases nanoparticle volume fraction decreases. This situation occurs due to mass diffusivity and depends on the nanoparticles concentration. Therefore, increasing Schmidt number reduces the nanoparticles volume fraction concentration as expected. From Fig. 7(b) the combined effect of *Sc* and *M* on the dimensionless microorganism profile follow the same trend as dimensionless nanoparticle volume fraction distributions. Figs. 8(a) and 8(b) present the influence of the bioconvection Schmidt number (*Sb*) and Péclet number (*Pe*) with magnetic field respectively. Physically, *Sb* parameter is defined as ν / D_m which relates the ratio of momentum diffusivity to diffusivity of microorganisms. As *Sb* >1 is used in this study, microorganism concentration in Fig. 8(a) is reduced due to momentum diffusivity exceeds microorganism diffusivity. This situation creates a significant difference between them and thus leads to a reduction in microorganism density number magnitudes, χ(η). Meanwhile, *Pe* number is defined

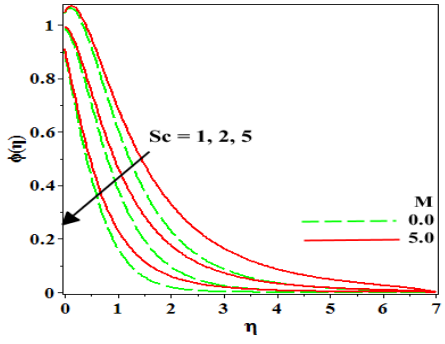

7(a)

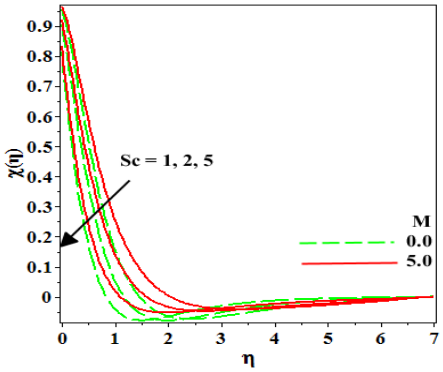

7(b)

Figure 7. The effects of the Sc and M on the dimensionless 7(a) nanoparticle volume fraction and 7(b) microorganisms when $Sb = 0.1,\ Pe = \lambda = 0.1,\ Rb = 0.1,$ and $\delta_u = \delta_v = \delta_T = \delta_C = \delta_n = 0.1.$

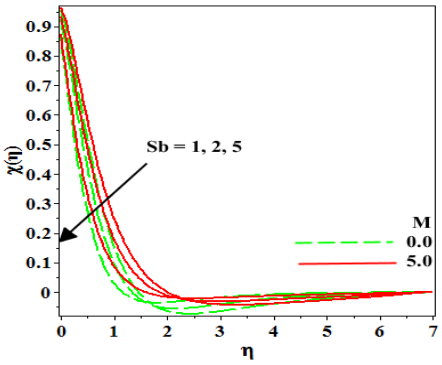

8(a)

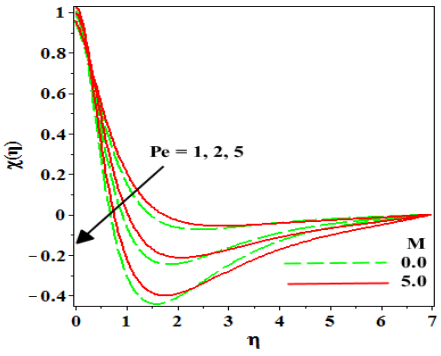

8(b)

Figure 8. Dimensionless microorganisms profile as a function of (a) the bio-convection Schmidt number with magnetic field and (b) the péclet number with magnetic field when $Sc = Pe = \lambda = Rb = 0.1,$ and $\delta_u = \delta_v = \delta_T = \delta_C = \delta_n = 0.1.$

as bW_C / D_m which relates the product of chemotaxis constant (b) and maximum microorganism swimming speed (W_C) to the diffusivity of microorganisms (D_m) in nanofluids. Therefore, higher *Pe* implies to the higher swimming speed of microorganisms and thus reduces microorganism concentration (see Fig. 8(b)). Based on the previous section, we have discussed the graphs plotted with respect to η for flow, temperature, nanoparticle volume fraction and microorganism concentration profiles. However, in reality application scientists and decision maker interested to investigate the characteristic of skin friction coefficient, heat transfer, mass transfer and microorganism transfer at the wall. Therefore, Table 2 and Table 3 summarize the effects of δ_u, δ_v, δ_T, δ_C and δ_n on the local skin friction in *x*-direction, local skin friction in *y* -direction, local Nusselt number, Sherwood number and number of motile microorganism without and with induced magnetic field respectively. For both cases (*M*=0 and *M*=1), the same pattern of local skin friction in *x*- and *y*-directions, local Nusselt number, Sherwood number and number of motile microorganism are observed as δ_u, δ_v, δ_T, δ_C and δ_n increase. It is found that $-f''(0)$ decreases with increasing of δ_u, δ_v and δ_T relatively weakly increases with increasing δ_C and δ_n. $-g'(0)$ is found to be increased with increasing δ_u, δ_C and δ_n. An enhancement effect of $-\theta'(0)$ also can be observed as δ_u, δ_C and δ_n increase. It has to be noted that δ_T plays an important roles to enhance $-\chi'(0)$ and reduce $-\theta'(0)$ with $-\phi'(0)$ significantly. Also, it seen that both $-\phi'(0)$ and $-\chi'(0)$ reduce as δ_C and δ_n increase respectively.

Table 2. Effect of multiple slips on physical quantities for non-magnetic flow (M=0).

Parameters									
δ_u	δ_v	δ_T	δ_C	δ_n	$-f''(0)$	$-g'(0)$	$-\theta'(0)$	$-\phi'(0)$	$-\chi'(0)$
0.0	0.1	0.1	0.1	0.1	1.06800	0.7588	2.0698	0.3941	0.4582
0.1	0.1	0.1	0.1	0.1	0.9477	0.7961	2.1279	0.4155	0.4668
0.2	0.1	0.1	0.1	0.1	0.8502	0.8250	2.1730	0.4316	0.4744
0.1	0.0	0.1	0.1	0.1	1.0365	0.8827	2.1416	0.4140	0.4775
0.1	0.2	0.1	0.1	0.1	0.8781	0.7268	2.1171	0.4168	0.4581
0.1	0.1	0.0	0.1	0.1	1.0348	0.8079	2.7229	0.7914	0.1685
0.1	0.1	0.2	0.1	0.1	0.8910	0.7882	1.7491	0.1760	0.6672
0.1	0.1	0.1	0.0	0.1	0.9464	0.7956	2.1277	0.4596	0.4329
0.1	0.1	0.1	0.2	0.1	0.9489	0.7964	2.1282	0.3791	0.4951
0.1	0.1	0.1	0.1	0.0	0.9446	0.7954	2.1274	0.4156	0.5228
0.1	0.1	0.1	0.1	0.2	0.9503	0.7966	2.1284	0.4154	0.4216

Table 3. Effect of multiple slips on physical quantities for magnetohydrodynamic flow (M=1).

Parameters									
δ_u	δ_v	δ_T	δ_C	δ_n	$-f''(0)$	$-g'(0)$	$-\theta'(0)$	$-\phi'(0)$	$-\chi'(0)$
0.0	0.1	0.1	0.1	0.1	0.7770	1.1018	2.0343	0.3941	0.4582
0.1	0.1	0.1	0.1	0.1	0.6753	1.1210	2.0756	0.4393	0.4047
0.2	0.1	0.1	0.1	0.1	0.5963	1.1355	2.1067	0.4510	0.4089
0.1	0.0	0.1	0.1	0.1	0.7666	1.2734	2.0892	0.4394	0.4135
0.1	0.2	0.1	0.1	0.1	0.6099	1.0029	2.0657	0.4393	0.3983
0.1	0.1	0.0	0.1	0.1	0.7583	1.1286	2.6387	0.7994	0.1176
0.1	0.1	0.2	0.1	0.1	0.6753	1.1210	2.0756	0.4393	0.4047
0.1	0.1	0.1	0.0	0.1	0.6741	1.1208	2.0753	0.4839	0.3708
0.1	0.1	0.1	0.2	0.1	0.6763	1.1211	2.0758	0.4023	0.4333
0.1	0.1	0.1	0.1	0.0	0.6727	1.1207	2.0751	0.4394	0.4506
0.1	0.1	0.1	0.1	0.2	0.6774	1.1212	2.0759	0.4392	0.3673

Conclusion

The unsteady MHD bioconvective anistropic slip flow of a nanofluid with microorganism past a rotating cone is studied as an initial study to investigate heat, mass and microorganism transfer in bio-chemical industrial which microfluidic devices involved. Similarity transformation technique is used to convert the two-dimensional momentum, temperature, nanoparticle volume fraction and microorganism equations into a set of ordinary differential equations which were then solved numerically. The effect of the selected governing parameters (δ_u, δ_v, δ_T, δ_C, δ_n, *Sc*, *Sb* and *Pe*) on the primary and secondary flows, temperature, nanoparticle concentration and density of motile microorganisms are described. Also, the values of the local skin friction in the *x*- and *y* -directions, local Nusselt numbers, Sherwood number and the motile microorganisms number are summarized in tables. The computations show that increasing *u*-slip velocity (δ_u) reduces primary local skin friction $-f''(0)$. Increasing *v*-slip velocity (δ_v) reduces secondary local skin friction. Also, increasing thermal slip, mass slip and microorganism slip strongly reduce heat, mass and microorganism transfer respectively.

Nomenclature

β_C	chemotaxis constant (m)
B	variable magnetic field strength (*tesla*)
B_0	constant magnetic field strength (*tesla*)
$C_{f\bar{x}}$	primary local skin friction coefficient
$C_{f\bar{y}}$	secondary local skin friction coefficient
C	nanoparticle volume fraction
C_w	wall nanoparticle volume fraction
C_0	nanoparticle volume fraction at origin
C_∞	ambient nanoparticle volume fraction
D	local thermal slip factor
D_B	Brownian diffusion coefficient $\left(\mathrm{m}^2/s\right)$
D_T	thermophoretic diffusion coefficient $\left(\mathrm{m}^2/s\right)$
D_n	microorganism diffusion coefficient $\left(\mathrm{m}^2/s\right)$
E	local mass slip factor
$f(\eta)$	dimensionless stream function
F	local microorganism slip factor

g gravitational acceleration $\left(\mathrm{m}/s^2\right)$

Gr -Grashoff number

k -thermal conductivity of the fluid $\left(W/mK\right)$

L characteristics length $\left(\mathrm{m}\right)$

m_w surface mass flux

M -magnetic field parameter

n number of motile microorganism

n_w wall motile microorganisms

n_0 number of motile microorganism at origin

n_∞ ambient motile microorganism

N_1 local primary velocity slip factor $\left(\mathrm{s}/\mathrm{m}\right)$

N_2 local secondary velocity slip factor $\left(\mathrm{s}/\mathrm{m}\right)$

Nb Brownian motion parameter

Nr buoyancy ratio parameter

Nt thermophoresis parameter

Nu_x local Nusselt number

Pe bio-convection Péclet number

Pr Prandtl number

q_w surface heat flux $\left(W/m^2\right)$

q_n surface micro-organism flux

Rb bioconvection Rayleigh number

Re_L^2 Rayleigh number

$\mathrm{Re}_{\bar{x}}$ Reynolds number

s unsteadiness parameter

Sb bio-convection Schmidt number

Sc Schmidt number

$Sh_{\bar{x}}$ local Sherwood number

$\bar{t}$ dimensional time $\left(s\right)$

t non-dimensional time

T nanofluid temperature $\left(K\right)$

T_0 temperature at origin $\left(K\right)$

T_w wall temperature $\left(K\right)$

T_∞ ambient temperature $\left(K\right)$

$\bar{u}$ velocity component along the $\bar{x}-$axis $\left(\mathrm{m}/s\right)$

$\bar{u}_w$ wall velocity $\left(\mathrm{m}/s\right)$

$\bar{u}_\infty$ free stream velocity $\left(\mathrm{m}/s\right)$

$\bar{v}$ velocity component along the $\bar{y}-$axis $\left(\mathrm{m}/s\right)$

$\bar{w}$ velocity component along the $\bar{z}-$axis $\left(\mathrm{m}/s\right)$

W_c maximum cell swimming speed $\left(\mathrm{m}/s\right)$

$\bar{x}$ dimensional coordinate along the $\bar{x}-$axis $\left(\mathrm{m}\right)$

$\bar{y}$ dimensional coordinate along the $\bar{y}-$axis $\left(\mathrm{m}\right)$

$\bar{z}$ dimensional coordinate along the $\bar{z}-$axis $\left(\mathrm{m}\right)$

Greek

α thermal diffusivity $\left(\mathrm{m}^2/s\right)$

α^* semi-vertical angle of the cone

β volumetric coefficient of expansion for temperature

$\chi(\eta)$ dimensionless number of motile microorganism

δ_u $u-$ velocity slip parameter

δ_v $v-$ velocity slip parameter

δ_T thermal slip parameter

δ_C mass slip parameter

δ_n microorganism slip parameter

$\phi(\eta)$ dimensionless nanoparticle volume fraction

η independent similarity variable

μ absolute viscosity of the fluid $\left(kg/ms\right)$

ν kinematic viscosity $\left(\mathrm{m}^2/s\right)$

$\theta(\eta)$ dimensionless temperature

ρ nanofluid density $\left(kg/m^3\right)$

σ variable electric conductivity $\left(siemens/m\right)$

Ω dimensionless angular velocity

τ ratio of the effective heat capacity of the nanoparticle

	material to the fluid heat capacity $\left(N/m^2\right)$	ψ	stream function $\left(\mathrm{m}^2/s\right)$
$\tau_{\overline{xz}}$	primary wall shear stress $\left(N/m^2\right)$	**Subscripts**	
		$(\,)'$	ordinary differentiation with respect to η.
$\tau_{\overline{yz}}$	primary wall shear stress $\left(N/m^2\right)$		

Acknowledgement:

The authors acknowledge financial support from Universiti Sains Malaysia, RU Grant 1001/PMATHS/81125.

References

[1] Anilkumar, D., Roy, S., Unsteady mixed convection flow on a rotating cone in a rotating fluid, *Appl. Math. Comput., 155*(2004), 2, pp. 545–561

[2] Nadeem, S., Saleem, S., Analytical study of rotating non-newtonian nanofluid on a rotating cone, *J. Thermophys. Heat Transf., 28*(2014), 2, pp. 295–302

[3] Nadeem, S., Saleem, S., Unsteady mixed convection flow of nanofluid on a rotating cone with magnetic field, *Appl. Nanosci., 4*(2014), pp. 405–414

[4] Hering, R. G., Grosh, R. J., Laminar free convection from a non-isothermal cone, *Int. J. Heat Mass Transf., 5*(1962), pp. 1059–1068

[5] Himasekhar, K., *et al.*, Laminar mixed convection from a vertical rotating cone, *Int Comm. Heat Mass Transf., 16*(1989), pp. 99–106

[6] Ravindran, R., *et al.*, Effects of injection (suction) on a steady mixed convection boundary layer flow over a vertical cone, *Int. J. Numer. Methods Heat Fluid Flow, 19*(2009), pp. 432–444

[7] Raju, S. H., Thermophoresis effect on heat and mass transfer from a rotating cone in a porous medium with thermal radiation, *Afrika Mat.*, (2016)

[8] Nadeem, S., Saleem, S., Analytical study of third grade fluid over a rotating vertical cone in the presence of nanoparticles, *Int. J. Heat Mass Transf., 85*(2015), pp. 1041–1048

[9] Hashmi, M.M., *et al.*, On the analytic solutions for squeezing flow of nanofluid between parallel disks, *Nonlinear Anal. Model. Control, 17*(2012), 4, 418–430

[10] Nadeem, S., Saleem, S., Analytical treatment of unsteady mixed convection MHD flow on a rotating cone in a rotating frame, *J. Taiwan Inst. Chem. Eng., 44*(2013), 4, pp. 596–604

[11] Kumar, A., Numerical study of effect of induced magnetic field on transient natural convection over a vertical cone, *Alexandria Eng. J., 55*(2016), 2, pp. 1211-1223

[12] Raju, C.S.K., Sandeep, N., Heat and mass transfer in MHD non-Newtonian bio-convection flow over a rotating cone/plate with cross diffusion, *J. Mol. Liq., 215*(2016), pp. 115–126

[13] Sulochana, C., *et al.*, Numerical investigation of chemically reacting MHD flow due to a rotating cone with thermophoresis and brownian motion, *86***(**2016**),** pp. 61–74.

[14] Saleem, S., Nadeem, S., Theoretical analysis of slip flow on a rotating cone with viscous dissipation effects, *J. Hydrodyn., 27*(2015), 4, pp. 616–623.

[15] Bataineh, K. Numerical and theoretical investigations of flow in a microcone and plate viscometer, *J. Fluids Eng., 136*(2014), 10, pp. 101201.

[16] Siddiqa, S., *et al.*, Numerical solutions of nanofluid bioconvection due to gyrotactic microorganisms along a vertical wavy cone, *Int. J. Heat Mass Transf. 101*(2016)**,** pp. 608–613

[17] Saleem, S., *et al.*, Buoyancy and metallic particle effects on an unsteady water-based fluid flow along a vertically rotating cone, *Eur. Phys. J. Plus, 129*(2014)**,** pp. 1–8 .

[18] Bandaru, M., *et al.*, Influence of nonlinear convection and thermophoresis on heat and mass transfer from a rotating cone to fluid flow in porous medium, *Therm. Sci., 00*(2016), pp. 4–4.

[19] Karniadakis, G., *et al.*, Microflows and nanoflows fundamentals and simulation, Springer Science & Business Media, New York, 2006.

[20] Xu, H.J., *et al.,* Analytical considerations of slip flow and heat transfer through microfoams in mini / microchannels with asymmetric wall heat fluxes, *Appl. Therm. Eng., 93*(2016), pp. 15–26.
[21] Kishore, N., Ramteke, R. R., Forced convective heat transfer from spheres to Newtonian fluids in steady axisymmetric flow regime with velocity slip at fluid-solid interface, *Int. J. Therm. Sci., 105*(2016), pp. 206–217
[22] Raza, J., *et al.,* Heat andmass transfer analysis of MHD nanofluid flow in a rotating channel with slip effects, *J. Mol. Liq., 219*(2016), pp. 703–708
[23] Uddin, J., *et al.,* Computational study of three-dimensional stagnation point nanofluid bio-convection flow on a moving surface with anisotropic slip and thermal jump effect, *J. Heat Transfer, 138*(2016), pp. 1–7
[24] Uddin, M.J., *et al.,* Finite element simulation of magnetohydrodynamic convective nanofluid slip flow in porous media with nonlinear radiation, *Alexandria Eng., J. 55*(2016), 2, pp. 1305–1319.
[25] Md Basir, M.F., *et al.,* Nanofluid slip flow over a stretching cylinder with Schmidt and Péclet number effects, *AIP Adv., 6*(2016), 5, pp. 055316
[26] Uddin, M.J., *et al.,* Lie group analysis and numerical solution of magnetohydrodynamic free convective slip flow of micropolar fluid over a moving plate with heat transfer, *Comput. Math. with Appl., 70*(2015), 5, pp. 846–856
[27] Turkyilmazoglu, M., Anomalous heat transfer enhancement by slip due to nanofluids in circular concentric pipes, *Int. J. Heat Mass Transf., 85*(2015), pp. 609–614
[28] Sinha, A., *et al.,* Peristaltic transport of MHD flow and heat transfer in an asymmetric channel : Effects of variable viscosity, velocity-slip and temperature jump, *Alexandria Eng. J., 54*(2015), 3, pp. 691–704
[29] Abdul Latiff, N.A., *et al.,* Unsteady forced bioconvection slip flow of a micropolar nanofluid from a stretching/shrinking sheet, J. of Nanomat. Nanoeng. and Nanosys, (2015) 1740349915613817
[30] Uddin, M.J., *et al.,* Multiple slips and variable transport property effect on magnetohydromagnetic dissipative thermosolutal convection in a porous medium, *J. Aerosp. Eng.,* (2014) 04016024
[31] Uddin, M.J., *et al.,* Scaling group transformation for MHD double-diffusive flow past a stretching sheet with variable transport properties taking into account velocity slip and thermal slip boundary conditions, *Pertanika J. Sci. Technol., 24*(2016), 1, pp. 53–70
[32] Bataineh, K.M., Taamneh, Y., Novel rotating cone viscous micro pump, *Int. J. Eng. Syst. Model. Simul., 5*(2013), 4, pp. 188–196
[33] Khan, W.A., Makinde, O. D., MHD nanofluid bioconvection due to gyrotactic microorganisms over a convectively heat stretching sheet, *Int. J. Therm. Sci., 81*(2014), pp. 118–124
[34] Nield, D.A., Kuznetsov, A.V., The Cheng–Minkowycz problem for the double- diffusive natural convective boundary layer flow in a porous medium saturated by a nanofluid, *Int. J. Heat Mass Transf., 54*(2011), pp. 374–378
[35] Shen, B., *et al*., Bioconvection heat transfer of a nanofluid over a stretching sheet with velocity slip and temperature jump, *Therm. Sci., 00*(2015)**,** pp. 128–128
[36] Sameh E. Ahmed, *et al.,* MHD Mixed Thermo-Bioconvection in Porous Cavity Filled by Oxytactic Microorganisms, *Therm. Sci., 00*(2017), pp. 1–12.
[37] Raju, C.S., Sandeep, N., Dual solutions for unsteady heat and mass transfer in bio-convection flow towards a rotating cone/plate in a rotating fluid, *Int. J. Eng. Res. Africa, 20*(2016), pp. 161–176.